Numerical modeling of wind turbine with vertical axis using turbulence model $k-\omega$ in ANSYS FLUENT

Muzaffar Hamdamov[1], *Bobir* Bozorov[2], *Hulkaroy* Mamataliyeva[3], and *Dilshod* Ergashov[1]

[1]Institute of Mechanics and Seismic Stability of Structures, Tashkent, Uzbekistan
[2]Samarkand State University Kattakorgan branch, Samarkand, Uzbekistan
[3]Uzbekistan State University of World Languages, Tashkent, Uzbekistan

Abstract. The paper considers a variant of the problem of modeling the flow around a developed wind turbine. Since the task is reduced to modeling a flat task, the 2D design mode was chosen. The $k-\omega$ turbulent model was used to model the vertical axis wind turbine. In the research process, experimental methods for measuring wind speed and torque, methods of mathematical modeling, and computational fluid dynamics were used. The object of research is a wind turbine designed to generate electricity from wind energy. The research aims to develop a wind turbine with a vertical axis and radial frames, equipped with flat blades and stoppers, operating at low wind speeds.
Research methods: in the research process, experimental methods for measuring wind speed and torque, methods of mathematical modeling, and computational hydrodynamics were used. A computational experiment HTBO with four sections based on the ANSYS environment was carried out. Scope of the results: the results will be used in designing and manufacturing wind turbines operating at low wind speeds. Ultimately, low-power wind turbines will be developed. Economic efficiency and significance of the work: the wind turbine being developed is made with available purchased materials and will have a short payback period. It is used for domestic and other purposes where access to electricity is limited.

1 Introduction

Large-scale work is underway in the Republic of Uzbekistan to support energy independence. Exploration work is being carried out to identify new fields, and measures are being taken to increase the development of oil and gas fields. They started building a nuclear power plant. The introduction of alternative renewable energy sources is gradually developing. Construction of solar and wind power stations has begun [1,2].

According to the Decree of the President of the Republic of Uzbekistan, No. PP-57 “On measures to accelerate the introduction of renewable energy sources and energy-saving technologies in 2023”, dated February 16, 2023, pretty tax and technical preferences are provided to individuals and legal entities that have installed renewable energy sources with a total capacity of up to 100 kW [3,4]. In general, by 2030, the development of a total wind power capacity of up to 5000 MW is predicted in Uzbekistan.

In numerous works, including [5,6], wind turbine aerodynamics was calculated using the ANSYS Fluent software package and other ready-made object-oriented packages. A complete three-dimensional model of the motion of an incompressible fluid based on the averaged Navier-Stokes equations according to Reynolds [7,8] and the finite volume method are used. The equations can be represented in primitive variables, in the Gromek-Lamb form [9, 10], and in other forms. At the same time, the weak point of these models is the lack of an adequate turbulence model because the mathematical models of turbulence tested on one or two tasks do not always give the correct result for other tasks, for example, under conditions of a tangential discontinuity, which occurs when studying wind turbines, and under conditions of anisotropic turbulence. Numerous results of theoretical testing of wind turbines have been produced in the ANSYS Fluent software package [11].

1.1 Equations for a moving frame of reference

Consider a coordinate system that moves with linear velocity and rotates at an angular speed relative to a stationary (inertial) frame of reference, as shown in Figure 1.

The main reason for using a moving frame is to present a non-stationary problem in a stationary (inertial) frame that is stable relative to the moving frame. For a stationary, moving frame of reference (for example, the rotation speed is constant), it is possible to transform the equations of fluid motion to a moving frame of reference so that stationary solutions are possible. It should also be noted that you can run a non-stationary simulation in a moving reference frame with a constant rotation rate. This would be necessary if you want to model, for example, the vortex shedding from a rotating fan blade. In this case, the instability is due to the natural instability of the fluid (formation of vortices) and not due to interaction with a stationary component. In ANSYS Fluent, moving a frame with non-stationary translational and rotational velocity motions is also possible. Again, the corresponding acceleration conditions are added to the equations of fluid motion. Such problems are inherently non-stationary concerning the moving coordinate system due to the non-stationary motion of the coordinate system.

The beginning of the moving system is determined by the position vector $\vec{r}_0$. The axis of rotation is determined by the unit direction vector $\hat{a}$ such that $\vec{\omega} = \omega\hat{a}$. The computational domain for the CFD problem is defined relative to the moving frame of reference in such a way that an arbitrary point in the CFD domain is defined by the position vector $\vec{r}$ from the start of the movement frame.

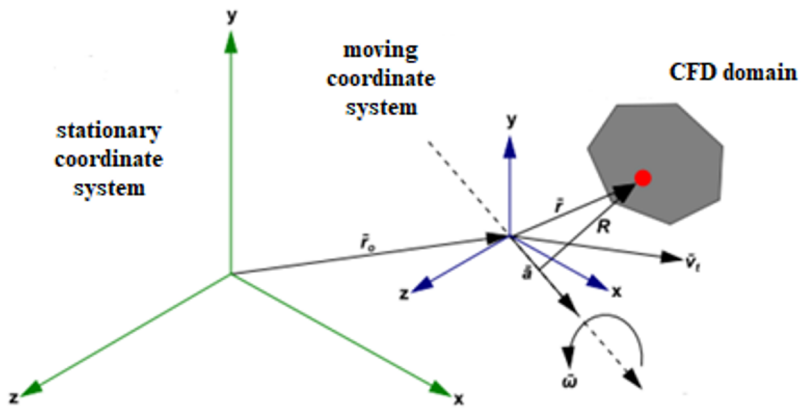

Fig. 1. Stationary and moving frames of reference

Fluid velocities can be converted from a fixed frame of reference to a moving frame using the following relations [4, 5]:

$$\vec{v}_r = \vec{v} - \vec{u}_r$$

Where

$$\vec{u}_r = \vec{v}_t + \vec{\omega} \times \vec{r}\,.$$

In the above equations $\vec{v}_r$ is relative speed (speed as seen from a moving reference frame), $\vec{v}$ is the absolute speed (the speed considered from a fixed frame of reference), $\vec{u}_r$ is the speed of the moving frame of reference relative to the inertial frame of reference, $\vec{v}_t$ is frame forward speed, $\vec{\omega}$ is angular velocity. It should be noted that both $\vec{\omega}$ and $\vec{v}_t$ can be functions of time.

When solving the equations of motion in a moving reference frame, the fluid acceleration is supplemented by additional terms that appear in the momentum equations [12, 13]. Moreover, equations can be written in two ways:

Expression of momentum equations using relative velocities as dependent variables (known as the relative velocity formulation).

Expression of momentum equations using absolute velocities as dependent momentum variables equations (known as the absolute velocity formulation).

The basic equations for these two formulations will be presented below. It may be noted here that pressure-based solvers in the ANSYS Fluent code used are allowed to use either of these two formulations, while density-based solvers always use the absolute velocity formulation [14, 15].

Relative Velocity Formulation. To formulate the relative velocity, the basic equations of fluid flow in a moving frame of reference can be written as follows:

Mass Conservation:

$$\frac{\partial \rho}{\partial t} + \nabla \rho \vec{v}_r = 0\,.$$

Conservation of momentum:

$$\frac{\partial}{\partial t}\left(\rho \vec{v}_r\right) + \nabla\left(\rho \vec{v}_r \vec{v}_r\right) + \rho\left(2\vec{\omega} \times \vec{v}_r + \vec{\omega} \times \vec{\omega} \times \vec{r} + \vec{\alpha} \times \vec{r} + \vec{a}\right) = -\nabla p + \nabla \bar{\bar{\tau}}_r + \vec{F}\,,$$

Where $\vec{\alpha} = \dfrac{d\vec{\omega}}{dt}$, $\vec{a} = \dfrac{d\vec{v}_t}{dt}$.

Energy saving:

$$\frac{\partial}{\partial t}\left(\rho E_r\right) + \nabla\left(\rho \vec{v}_r H_r\right) = \nabla\left(k\nabla T + \bar{\bar{\tau}}_r \vec{v}_r\right) + S_h.$$

The momentum equation contains four additional acceleration conditions. The first two terms are Coriolis acceleration and centripetal acceleration respectively. These terms appear

both for constantly moving frames of reference (that is, and are constant) and for accelerating frames of reference (that is, and/or are functions of time). The third and fourth terms are due to the non-stationary change in the rotation speed and linear speed, respectively. These terms disappear for constant rates of travel and/or rotation. In addition, viscous stress is an identical stress tensor $(\bar{\bar{\tau}}_r)$ given by someone

$$\bar{\bar{\tau}} = \mu\left[\left(\nabla\vec{v} + \nabla\vec{v}^{T}\right) - \frac{2}{3}\nabla\vec{v}I\right];$$

where μ is molecular viscosity, *I* is unit tensor, and the second term on the right side equals the volume dilation effect.
Except that relative velocity derivatives are used. The energy equation is written regarding relative internal energy and relative total enthalpy, also known as rotalpia. These variables are defined as:

$$E_r = h - \frac{p}{\rho} + \frac{1}{2}\left(v_r^2 - u_r^2\right), \;\; H_r = E_r + \frac{p}{\rho}.$$

Formulation of absolute speed. To formulate the absolute velocity, the basic equations of fluid flow for a constantly moving frame of reference can be written as follows [16, 17]:
Mass Conservation:

$$\frac{\partial\rho}{\partial t} + \nabla\rho\vec{v}_r = 0\cdot$$

Conservation of momentum:

$$\frac{\partial}{\partial t}\left(\rho\vec{v}_r\right) + \nabla\left(\rho\vec{v}_r\vec{v}\right) + \rho\left(\vec{\omega}\times\left(\vec{v} - \vec{v}_t\right)\right) = -\nabla p + \nabla\bar{\bar{\tau}} + \vec{F};$$

Energy saving [18, 19]:

$$\frac{\partial}{\partial t}\left(\rho E\right) + \nabla\left(\rho\vec{v}_r H + p\vec{u}_r\right) = \nabla\left(k\nabla T + \bar{\bar{\tau}}\vec{v}\right) + S_h.$$

In this formulation, the Coriolis acceleration and the centripetal acceleration are simplified to one term $\left(\vec{\omega}\times\left(\vec{v} - \vec{v}_t\right)\right)$. Note that the momentum equation for formulating absolute velocity does not contain explicit terms, including $\vec{\alpha}$ and $\vec{a}$.

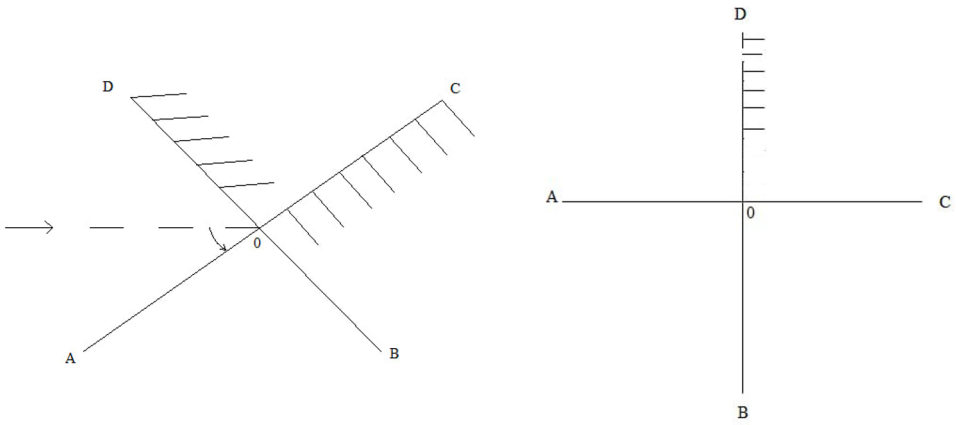

(b) *(a)*

Fig. 2. Positions of blades when device rotates around its axis

Let's discuss our object of study from the point of view of mathematical modeling of a moving element.

The windward blades rest against the frame, and the leeward blades parallel the wind speed vector. When viewed from above, the device rotates counterclockwise. Then, in position (a), the OB blades are on the windward side and make up 90 degrees with the wind, i.e., take full wind energy.

Disconnection of the AC from the direction of the wind occurs, as already noted, counterclockwise. If the deflection angle is α, then the action of the wind to the blades of the OA section is $\sin\alpha$, and the blade of the OB section $-\cos\alpha$. The first of these quantities is increasing, and the second is decreasing. The blades of the OC and OD sections, which move against the flow, take a neutral position under the influence of the wind - they become parallel to the wind speed vector.

However, the effect of the wind on sections with neutral blades that are upwind will also be noticeable. As noted in the part of the patent description, the difference in the moments of the windward (working) and leeward (neutral) blades organizes the device's rotation around its axis. It leads to the rotation of the axis of the electric generator.

Thus, when modeling an object, it is necessary to consider that the windward blades resting on the frame make the same movement as the frame, which corresponds to the formulation of the absolute speed. At the same time, the lee blades adjust to the direction of the wind and form a variable angle relative to the section frame.

Based on these judgments, it is necessary to set the task on ANSYS Fluent for conducting the calculation.

Relative reference frame motion specification [7]

ANSYS Fluent allows you to specify a motion reference frame relative to an already moving (rotating and moving) frame of reference. In this case, the resulting velocity vector is calculated as

$$\vec{v}_r = \vec{v} - \vec{u}_r$$

where $\vec{u}_r = \vec{u}_{r1} + \vec{u}_{r2}$ and $\vec{\omega} = \vec{\omega}_1 + \vec{\omega}_2$.

The rotation vectors are added together as in the equation $\vec{\omega} = \vec{\omega}_1 + \vec{\omega}_2$, since the motion of the frame of reference can be considered as a rotation of a rigid body, where the

rotation speed is constant for every point of the body. In addition, this allows the rotation to be formulated as an axial angular velocity vector (also known as pseudo), describing infinitesimal instantaneous transformations. In this case, both rotation speeds obey the commutative law. It should be noted that this approach is not sufficient when working with finite rotations. In this case, it is necessary to formulate rotation matrices based on Euler angles.

Technology and methodology of CFD: Computational Fluid Dynamics or CFD (from the English Computational Fluid Dynamics) includes the analysis of fluid flow, heat transfer, and related systems using computer simulations. It has a wide range of industrial and non-industrial applications and is a reliable product manufacturing tool. It is widely used in the automotive industry to predict a vehicle's drag and lift forces. Computational fluid dynamics requires significant knowledge of fluid dynamics, mathematics, and programming. It involves accepting a wide range of variables to create models that can reflect the necessary needs of a real system.

Computational fluid dynamics is used to study aircraft and vehicles. This is useful when analyzing the lift and drag of a vehicle. Using this method, one can easily investigate the hydrodynamics of ships. Using this technique, one can easily study combustion processes in internal combustion engines and gas turbines of industrial power plants, flows in rotating channels, and diffusers of turbomachines. In biomedical engineering, it is used to analyze blood flow through veins and arteries. It is also used for weather forecasting in meteorology. Modern ecologists also use this method to determine the distribution of wastewater and pollutants.

Industrial companies are very happy with computational fluid dynamics because it offers unique advantages over experiment-based methods for designing fluid or flow systems. It allows for unlimited levels of detail in results and helps improve fluid systems. This significantly reduces lead times and costs for new system designs. CFD facilitates system analysis where it is difficult to work with managed systems. It also can examine systems under emergency conditions at their normal operating level and beyond. In experimental studies, the costs of hiring staff and other aspects vary; therefore, industries increasingly ignore experiments. On the other hand, computational fluid dynamics gives a huge amount of results at no additional cost and is very cheap to implement.

Fluid flow problems can be solved using CFD codes (software packages). These codes are based on numerical algorithms and provide easy access to complex fluid flow problems. CFD codes consist of a preprocessor, a solver, and a postprocessor.

To date, a large number of commercial and non-commercial CFD packages have been implemented [7]:

- Altair Hyperworks
- ANSYS (Fluent and CFX)
- Autodesk CFD
- CFL3D
- COMSOL Multiphysics;
- FLOW-3D
- FlowVision
- FUN3D
- NUMECA OMNIS
- OpenFOAM
- PHOENICS
- Siemens STAR-CCM+
- SimScale
- SOLIDWORKS Flow Simulation
- SU2

Entering a fluid problem into a CFD program to convert it to a simple part enters the preprocessing context. This includes defining the geometry of a particular area, i.e., the computing area. In addition, it is divided into several smaller, non-overlapping subregions in a grid or cell grid pattern. It helps in defining and modeling fluid properties. The solution for variables such as temperature, pressure, etc., is determined at the nodes of each grid. The accuracy of any CFD solution is determined by the number of cells in the grid since the greater the number of cells or grids, the higher the accuracy of the solution. The mesh size depends on the system's high cost and the solution's accuracy.
The finite difference method, finite element method, and spectral method are the three main numerical solution methods, of which the finite volume method is mainly used. The numerical algorithm includes the integration of the basic equations of fluid flow over all finite volumes of the domain. The resulting integral equations are then transformed into a system of algebraic equations. Then the algebraic equations are solved by the iterative method. The main difference between the finite volume method and other CFD methods is integrating the control volume into the finite volume method. The resulting equations have the same properties for each cell of finite size. This simple concept makes it easier for engineers to understand fluid flow than other methods. Conservation of various flow variables, such as enthalpy and the velocity within the final control volume, is expressed to evaluate whether it is increasing or decreasing. CFD codes consist of discretization methods that are useful for convection, diffusion, and other key transport phenomena.
The ever-increasing popularity of CFD software has expanded processing capabilities. This facilitated greater graphical possibilities along with domain geometry and grid display. The CFD software package now includes vector plots, line and hatched contour plots, contour postscript output, and particle tracking. These features are complemented by the animated and dynamic display of results. This made it possible to transfer ideas to people who did not have an engineering background.

Fluid flow problems are built on complex sets of physical, chemical, and mathematical concepts, and experienced specialists are required to master them. The user must have considerable knowledge of various subjects before modeling CFD tasks. The user must be able to identify and formulate the chemical and physical aspects of a flow problem. The key decisions made in fluid flow simulations are the effect of ambient temperature, air density changes, turbulent flow, air bubbles, etc. When modeling equations, it is necessary to make the right decisions to maintain the fluid problem's desired characteristics. Accuracy when simplifying the equation improves the quality of the CFD. A detailed description of the domain geometry and mesh design is critical at an early stage to obtain successful simulation results. Successful modeling can be obtained through convergence and mesh dependence. A convergent solution can be achieved by choosing different acceleration devices and relaxation factors.

2 Methods

The paper considers a variant of the problem of modeling the flow around a developed wind turbine.

Building a CAD model Fig. 3. was carried out in the SolidWorks environment, where the main geometric dimensions were specified. Since the task is reduced to modeling a flat task, the 2D design mode was chosen.

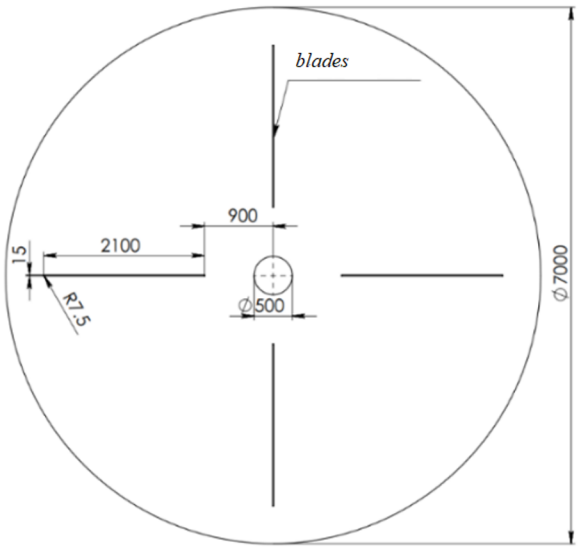

Fig. 3. 2D wind turbine geometry (top view)

In the process of solving the problem, one turbulence model can be used to describe turbulence.

Model $k-\omega$ this model is historically the very first high-Reynolds model with two differential equations [7, 20-23]:

$$\begin{cases} \dfrac{\partial}{\partial t}(\rho k)+\dfrac{\partial}{\partial x_i}(\rho k u_i)=\dfrac{\partial}{\partial x_j}\left[\Gamma_k \dfrac{\partial k}{\partial x_j}\right]+G_k-\rho\beta^* f_{\beta^*} k\omega+S_k, \\ \dfrac{\partial}{\partial t}(\rho \omega)+\dfrac{\partial}{\partial x_i}(\rho \omega u_i)=\dfrac{\partial}{\partial x_j}\left[\Gamma_\omega \dfrac{\partial \omega}{\partial x_j}\right]+G_\omega-\rho\beta f_\beta \omega^2+S_\omega. \end{cases}$$

Does not contain terms reflecting the effect of molecular viscosity on turbulence. Now rarely used. Turbulent eddy viscosity is calculated by the formula: $\mu_t=\alpha^*\dfrac{\rho k}{\omega}$, model constants are defined as a function $\Gamma_k=\mu+\dfrac{\mu_t}{\sigma_k}$, $\Gamma_\omega=\mu+\dfrac{\mu_t}{\sigma_\omega}$,

$\alpha^*=\alpha^*_\infty\left(\dfrac{\alpha^*_0+\mathrm{Re}_t/R_k}{1+\mathrm{Re}_t/R_k}\right)$, $\mathrm{Re}_t=\dfrac{\rho k}{\mu\omega}$, $G_k=-\rho\overline{u_i'u_j'}\dfrac{\partial u_j}{\partial x_i}$, $\Omega_{ij}=\dfrac{1}{2}\left(\dfrac{\partial u_i}{\partial x_j}-\dfrac{\partial u_j}{\partial x_i}\right)$,

$G_\omega=\alpha\dfrac{\omega}{k}G_k$, $\alpha=\dfrac{\alpha_\infty}{\alpha^*}\left(\dfrac{\alpha_0+\mathrm{Re}_t/R_\omega}{1+\mathrm{Re}_t/R_\omega}\right)$, $\chi_k\equiv\dfrac{1}{\omega^3}\dfrac{\partial k}{\partial x_j}\dfrac{\partial \omega}{\partial x_j}$,

$\beta^*=\beta_i^*\left[1+\zeta^* F(M_t)\right]$.

Cosure constants for $k-\omega$ model:

$$\alpha_0^* = \frac{\beta_i}{3},\ \mathrm{R}_k = 6,\ \beta_i = 0.072,\ \alpha^* = \alpha_\infty^* = 1,\ R_\omega = 2.95,\ \alpha = \alpha_\infty = 1,$$

$$\beta_i^* = \beta_\infty^* \left(\frac{4/15 + \left(\mathrm{Re}_t / R_\beta\right)^4}{1 + \left(\mathrm{Re}_t / R_\beta\right)^4} \right),\quad \zeta^* = 1.5,\quad R_\beta = 8,\quad \beta_\infty^* = 0.09,$$

$$\chi_\omega = \left| \frac{\Omega_{ij}\Omega_{ij}S_{ij}}{\left(\beta_\infty^*\omega\right)^3} \right|,\quad \beta = \beta_i \left[1 - \frac{\beta_i^*}{\beta_i}\zeta^* F\left(M_t\right) \right],\quad M_t^2 \equiv \frac{2k}{a^2},\quad M_{t0} = 0.25,$$

$$a = \sqrt{\gamma RT},\ \alpha_\infty^* = 1,\ \alpha_\infty = 0.52,\ \alpha_0 = \frac{1}{9},\ \beta_\infty^* = 0.09,\ \beta_i = 0.072,\ R_\beta = 8,$$

$$R_k = 6,\ R_\omega = 2.95,\ \zeta^* = 1.5,\ M_{t0} = 0.25,\ \sigma_k = 2.0,\ \sigma_\omega = 2.0.$$

3 Results and Discussion

Calculation grid. Next, the CAD model was exported to Cadence Pointwise to create a hybrid finite volume mesh. An O-grid topology type was chosen to define the CFD flow domain. The input velocity boundary condition was specified in the I first quarter of the circular domain and in the remaining parts of the atmospheric pressure output condition. Also, cell layers were allowed directly at the blade walls to accurately model the turbulent viscous layer, where $Y+<4$.

Type - unsteady incompressible flow in the 2D formulation. The mass of the installation is 72 kg, and the moment of inertia along the Z axis is 90 kg·m^2.

The results of calculating the drag coefficient from the angular position of the first blade when using $k-\omega$ turbulence models are compared with experimental data (Figure 4).

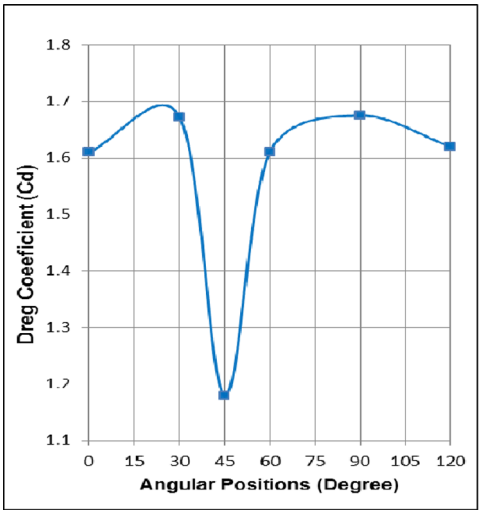

Fig. 4. Dependence of drag coefficient from angular position of first blade

The results of modeling the rotation of the wind turbine blades showed a speed of 25-30 rpm with a wind speed of 8 m/s (see Figure 4).

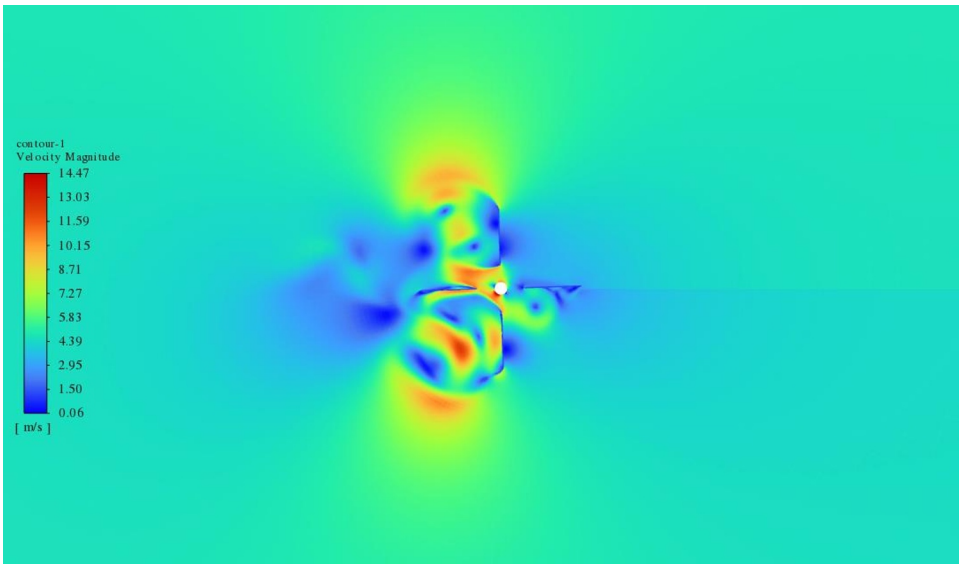

Fig. 5. Speed Loop V=8 m/s. $k-\omega$ model

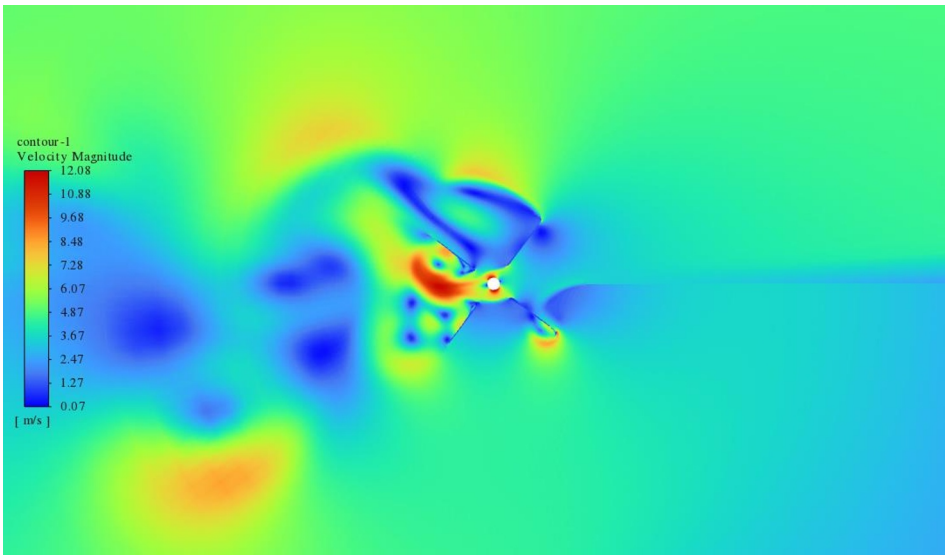

Fig. 6. Contour of rotation speed V=5 m/s. $k-\omega$ model

4 Conclusions

Numerous results on the aerodynamics of the HTBO have been obtained, which should be further processed by statistical methods and analyzed.
Theoretical calculations in the ANSYS environment have established that when calculating the aerodynamics of the proposed HTTO, one can use turbulence models $k-\omega$, which

more adequately describe the flow process around a rotating device.
Primary experimental results have been obtained, showing that at wind speeds above 5 m/s, the developed device can provide 0.7 kW of energy.
The results on the aerodynamics of the HTBO, which are not included in this report, must be further processed by statistical methods and analyzed.

References

1. Global Wind Report 2019 | Global Wind Energy Council.
2. Wind energy in Europe in 2019 (англ.) // WindEurope. – 2020. – С. 18-19.
3. Dan-mei Hu , Hong-lei Ding .Numerical simulation of the near-wake flow field of a horizontal-axis wind turbine (HAWT) model // Journal of Vibroengineering, Vol. 18, Issue 5, 2016, p. 3258-3268. https://doi.org/10.21595/jve.2016.16934
4. Ponyatov A. Having entered the era of electricity // Science and life. - 2020. - No. 1. - P. 16.
5. Alan Wyatt, Electric Power: Challenges and Choices, (1986), Book Press Ltd., Toronto, ISBN 0-920650-00-7.
6. Naji Abdullah Mezaal, Osintsev K. V., Alyukov S.V. The computational fluid dynamics performance analysis of horizontal axis wind turbine // International Journal of Power Electronics and Drive System (IJPEDS) Vol. 10, No. 2, June 2019, pp. 1072~1080, DOI: 10.11591/ijpeds.v10.i2.pp1072-1080
7. Fluent, ANSYS FLUENT 12.0 Theory Guide, ANSYS Inc., April 2009, Sections 18.1.1 and 18.1.2
8. Jorn Madslien. Floating wind turbine launched, BBC NEWS, London: BBC, C. June 5 2009. Архивировано 26 января 2022 года. Дата обращения: 30 января 2023.
9. Annual installed global capacity 1996-2011.
10. Qiuyun Mo, Jiabei Yin , Lin Chen, Weihao Liu , Li Jiang, and Zhiqiang Liao. Numerical Simulation of Aerodynamic Performance of Off-grid Small Vertical Axis Wind Turbine // E3S Web of Conferences 53, 02004 (2018) https://doi.org/10.1051/e3sconf/20185302004 ICAEER 2018
11. J. W. Bin. “Research on aerodynamics of H-type vertical axis wind turbine.” Chongqing University(2016)
12. Kuik, G.A.M., the Lanchester-Betz-Joukowsky Limit, Wind Energy 10, 2007, 10, pp. 289-291.
13. G. K. Batchelor. An Introduction to Fluid Dynamics. Cambridge Univ.Press. Cambridge, England. 1967.
14. R. D. Rauch, J. T. Batira, and N. T. Y. Yang. Spatial Adaption Procedures on Unstructured Meshes for Accurate Unsteady Aerodynamic Flow Computations // Technical Report AIAA-91-1106. AIAA. 1991.
15. Roach P. Computational fluid dynamics. – M.: Mir, 1980. – 616 p.
16. Anderson D., Tannehill J., Pletcher R. Computational fluid mechanics and heat transfer: In 2 volumes. Per. from eng. - M ..: Mir, 1990. - S. 728 (1st volume 392 p.).
17. Patankar S. Numerical methods for solving problems of heat transfer and fluid dynamics. Translated from English. – M.: Energoatomizdat, 1984. – 152 p.
18. Hamdamov M.M. Simulation and modeling of flow field around a horizontal axis wind turbine. ICISCT 2022 conference is technically sponsored by ieee and IEEE photonics

society. 28th, 29th and 30th of september 2022, Tashkent, Uzbekistan

19. Hamdamov M.M., Ishnazarov A.I., Mamadaliev Kh.A. Numerical modeling of vertical axis wind turbines using Ansys Fluent software // NEW2AN 2022, LNCS 13772, pp. 156–170, 2023. https://doi.org/10.1007/978-3-031-30258-9_14
20. Fayziev, R.A., Hamdamov, M.M. Model and program of the effect of incomplete combustion gas on the economy. In: ACM International Conference Proceeding Series, pp. 401–406 (2021) https://doi.org/10.1145/3508072.3508147
21. Khujaev, I.K., Hamdamov, M.M.: Axisymmetric turbulent methane jet propagation in a co-current air flow under combustion at a finite velocity. Herald of the Bauman Moscow State Technical University, Series Natural Sciencesthis link is Disabled, no. 5, pp. 89–108 (2021) https://doi.org/10.18698/1812-3368-2021-5-89-108
22. Hwang I S, Min S Y, Jeong I O. Efficiency Improvement of a New Vertical Axis Wind Turbine by Individual Active Control of Blade Motion. School of Mechanical & Aerospace Engineering, Korea, 2005.
23. Zuo Wei, KANG Shun, Qiu Yongxing, et al. Numerical Simulation of The Aerodynamic Performance of H Type Wind Turbine. Engineering Thermophysics [J], 2013, 34(8): 1462-1465.